Available online at www.sciencedirect.com

SciVerse ScienceDirect

Ceramics International 38 (2012) 1479–1487

CERAMICS INTERNATIONAL

www.elsevier.com/locate/ceramint

Cleaner production of porcelain tile powders. Fired compact properties

Z. Shu [a,b,*], J. Garcia-Ten [b], E. Monfort [b], J.L. Amoros [b], J. Zhou [c], Y.X. Wang [a]

[a] MOE Key Laboratory of Biogeology and Environmental Geology and School of Environmental Studies, China University of Geosciences, 430074 Wuhan, PR China

[b] Instituto de Tecnología Cerámica, Asociación de Investigación de las Industrias Cerámicas, Universitat Jaume I, 12006 Castellón, Spain

[c] MOE Key Engineering Research Center of Nano-Geomaterials and Faculty of Material Science and Chemical Engineering, China University of Geosciences, 430074 Wuhan, PR China

Received 13 August 2011; accepted 13 September 2011
Available online 17 September 2011

Abstract

A new ceramic powder preparation process, the droplet-powder granulation process (DPGP), was recently proposed for the cleaner production of ceramic tiles. The DPGP granules and resulting pressed compacts were characterized and compared with the granules and compacts obtained by spray-drying (SD) and dry granulation (G) processes in a previous paper. The results showed the feasibility of using the DPGP in the pre-firing stage of porcelain tile manufacture.

This study compares the firing behaviour and fired properties of compacts pressed from three different types of granulated powders: DPGP, SD, and G and from a non-granulated powder (NG) obtained by dry milling. The evolution of compact microstructure (porosity and pore size distribution) with firing temperature was monitored and the fired compact properties (bulk density, water absorption, and stain resistance) were determined.

The study shows that the DPGP improved the sintering behaviour and final properties of the resulting porcelain tiles with respect to those obtained by the G process. However, the fired compacts prepared from the DPGP powder exhibited a higher porosity and pore size compared with those of the compacts obtained from the SD granules at the same pressing pressure. The results obtained open up the possibility of manufacturing glazed porcelain tiles with a more eco-friendly process. However, the results also indicate that polished porcelain tile manufacture by the DPGP requires further research in order to improve granule characteristics, in particular green granule deformability, which is the critical factor in porcelain tile densification and vitrification during firing.

Keywords: A. Pressing; A. Sintering; B. Porosity; B. Microstructure-final; D. Porcelain; Tiles

1. Introduction

Porcelain tile is a ceramic product that displays excellent performance with regard to mechanical strength and frost, stain, and chemical resistance. These features are closely related to the porous microstructure of the fired tile [1], which stems from the evolution of green tile microstructure during heat treatment [2–5]. As temperature rises, liquid-phase formation (beginning at about 900 °C) increases, bringing the particles closer together, lowering total porosity, and altering pore size and shape. Sufficiently high temperatures (above 1180 °C) close the pores and reduce apparent porosity. However, excessively high temperatures raise the gas pressure in the closed pores above the capillary pressure, which leads to bloating.

At present, porcelain tile is predominantly manufactured by the dry pressing of ceramic powder. The porous microstructure of the green tile is essentially determined by powder properties and pressing conditions. Under constant industrial pressing conditions (moisture content typically between 0.05 and 0.065 kg water/kg dry solid and pressing pressure between 35 and 45 MPa) [1], powder properties, which depend on the raw materials preparation process, are the major factor in determining green tile microstructure.

A novel raw materials preparation process, the droplet-powder granulation process (hereafter DPGP) based on the wet milling of the raw materials and a new granulation method, was

* Corresponding author at: MOE Key Laboratory of Biogeology and Environmental Geology and School of Environmental Studies, China University of Geosciences, 430074 Wuhan, PR China.

E-mail addresses: zhushu426@gmail.com, zhushu426@163.com (Z. Shu).

0272-8842/$36.00
doi:10.1016/j.ceramint.2011.09.031

recently proposed for cleaner production of ceramic powders compared with the widely used spray-drying process, since it significantly reduces particulate matter emissions into the air (98%), energy consumption (24%), and water consumption (69%) [6]. The properties of the DPGP powder and resultant pressed green compacts were studied in a previous paper [7]. The study demonstrated the feasibility of using the DPGP in the pre-firing stage of porcelain tile manufacture.

The present study analyses the firing behaviour and fired properties of compacts formed by pressing from the DPGP powder, in comparison with those of compacts pressed from powders obtained by other preparation processes, namely wet milling and spray drying (hereafter SD), dry milling and granulation (hereafter G), and dry milling without granulation (hereafter NG or non-granulated powder).

2. Experimental

2.1. Raw materials and powder preparation

A standard porcelain tile composition was used to prepare four different types of powder: three granulated powders (SD, DPGP, and G) and one non-granulated powder (NG). The raw materials, composition, and processing methods used to prepare the four powders have been described elsewhere in a previous paper [7].

2.2. Pressing and firing of the compacts

The four test powders were moistened (0.055 kg water/kg dry solid) and stored for 24 h before pressing. A uniaxial press with a cylinder die of 40 mm diameter was used to press the test disks.

Two series of test compacts were prepared, based on the typical pressing conditions used in industry for SD powder (pressing pressure: 32.5 MPa, dry bulk density: 2.00 g/cm^3). In the first series, dry bulk density was kept constant at 2.00 g/cm^3; in the second, pressing pressure was held at 32.5 MPa for the four powders. Table 1 details the pressing conditions.

The green compacts were dried at 110 °C to constant weight and fired in a laboratory electric kiln at different peak temperatures, ranging from 1000 to 1240 °C. The heating rate was 25 °C/min and the hold time at peak temperature was 6 min.

2.3. Characterization of the compacts

The porous microstructure of the unfired compacts and of the compacts fired at relatively low temperatures (up to 1100 °C) was characterized by determining bulk density (BD) by mercury displacement, absolute density by a helium pycnometer (Quantachrome Ultrapycnometer 1000), and pore size distribution by mercury porosimetry (Micromeritics AutoPore III using about 2 g sample and a 130° contact angle). True porosity was calculated from the bulk density and absolute density data.

The pore size distributions were fitted to log-normal distributions and the values of d_{16}, d_{50}, and d_{84} (representative of the large, medium, and small pore fractions, respectively) were determined [3,8,9].

Table 1
Pressing conditions used to form the test compacts.

Powder	Series 1 (pressed to a dry bulk density of 2.00 g/cm^3) Pressure applied (MPa)	Series 2 (pressed at a pressure of 32.5 MPa) Resultant dry bulk density (g/cm^3)
SD	32.5	2.001 ± 0.002
DPGP	29.0	2.020 ± 0.002
G	15.5	2.094 ± 0.001
NG	[a]	1.868 ± 0.005

[a]The required pressure exceeded the maximum pressure of the lab press (65 MPa).

The compacts fired at high temperatures (1180–1240 °C) were characterized by determining bulk density (BD) by mercury displacement and water absorption (WA) according to standard UNE-EN ISO 10545-3.

In order to determine their stain resistance, the fired compacts were polished using diamond abrasive to size 1 μm. The polished surfaces were observed in an optical microscope with the bright field signal (BF). The chromatic coordinates (L^*, a^*, and b^*) were determined on the polished compacts with a diffuse reflectance spectrophotometer, using a CIE 10° standard observer and CIE standard illuminant D65. The polished surfaces of the compacts were then painted with a permanent (a) rubbing with a water-dampened cloth; (b) rubbing with a cloth impregnated with ethanol for 3 min at a set pressure of 0.8 kg/cm^2 (equivalent to strong manual pressure) by a mechanical device rotating constantly at 180 rpm.

The chromatic coordinates were then measured again after applying the above cleaning methods. Initial and final dirt retention were assessed as the colour difference ΔE^* [3,10] of the polished compact before staining and after cleaning by the (a) method and (b) method, respectively. ΔE^* was calculated from the following equation:

$$\Delta E^* = \sqrt{\left(L_0^* - L^*\right)^2 + \left(a_0^* - a^*\right)^2 + \left(b_0^* - b^*\right)^2}$$

where L_0^*, a_0^*, b_0^* and L^*, a^*, b^* are the compact chromatic coordinates before staining and after cleaning, respectively.

The larger the value of ΔE^*, the harder it was to clean the compact.

3. Results and discussion

3.1. Compacts pressed to constant dry bulk density (2.00 g/cm^3)

3.1.1. Evolution of compact microstructure with firing temperature

Fig. 1 plots the pore size distributions of the unfired SD, DPGP, and G compacts and of the SD, DPGP, and G compacts fired at different temperatures (1000, 1050, and 1100 °C). Table 2 details the true porosity of the test pieces.

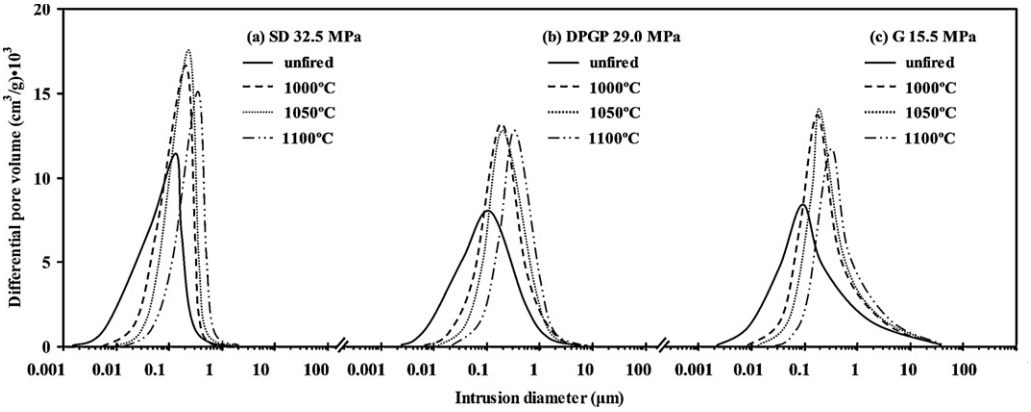

Fig. 1. Pore size distribution of the unfired and fired (a) SD, (b) DPGP, and (c) G compacts pressed at different pressures (32.5, 29.0, and 15.5 MPa respectively) to constant dry bulk density (2.00 g/cm^3).

Fig. 1 and Table 2 show that, for the SD compacts, when temperature increased porosity decreased (Table 2), the porosity distribution curve progressively shifting towards larger pore sizes, i.e. the pores grew (Fig. 1a). When the compacts were fired to 1000 °C, the increase in true porosity (shown in Table 2) occurred as a result of the loss on ignition (decomposition of clay minerals, organic matter, etc.), which raised porosity [11], and limited compact sintering owing to the small quantity of liquid-phase formation at low temperatures.

This is consistent with previous studies [3,12,13] on ceramics and glasses: in clayey or glassy materials with a broad initial pore size distribution, liquid-phase formation in firing leads to preferential elimination of the smaller pores, particle rearrangement with ensuing differential shrinkage of the material, and growth of the larger pores. This occurs because, when pore size decreases, the capillary pressure increases, causing the arising liquid phase to push the solid particles closer together, eliminating the smaller pores and enlarging the larger ones.

The same trend was found in the DPGP (Fig. 1b) and G (Fig. 1c) compacts, owing to the existence of a broad pore size distribution in the unfired compacts.

In order to analyse the influence of the powder preparation process on the porosity of the fired compacts, the pore size distributions of the SD, DPGP, and G compacts fired at 1100 °C were plotted together in Fig. 2a. The figure shows that the pore size distributions of these three compacts were identical in the small-pore fraction (<0.4 μm), but quite different in the medium-pore (0.4–1 μm) and large-pore (1–10 μm) fractions. The SD compact exhibited the narrowest pore size distribution and the lowest large-pore fraction, whereas the G compact displayed the widest pore size distribution and the highest large-pore fraction. The DPGP compact exhibited a pore size distribution and large-pore fraction intermediate between those of the SD and G compacts. The same trend was found in the pore size distributions of the compacts fired at 1000 °C and 1050 °C (figures omitted).

The differences observed in the pore size distribution at 1100 °C (Fig. 2a) stemmed from the pre-existing differences in the unfired compacts, as may be observed in Fig. 2b, indicating that the powder preparation process, which is responsible for granule and unfired compact microstructure [7], significantly affects the pore size distribution of the fired compacts.

In order to analyse the influence of the powder preparation process on the evolution of pore size distribution during sintering, the values of d_{16}, d_{50}, and d_{84} of the compacts were plotted versus firing temperature in Fig. 3. The figure shows that there was very little or no difference in the pore size of the unfired compacts and in the pore growth rate (slope of the curves) of the small (d_{84}) and medium (d_{50}) pores. However, the pore growth rate of the large pores (d_{16}) differed, depending on the powder preparation process involved.

The growth rate of the large pores (d_{16}) was lowest in the SD compact, intermediate in the DPGP compact, and largest in the G compact. The same trend also existed in the values of d_{16} in the unfired compacts, indicating that the pore growth rate depended significantly on the pore size of the unfired test pieces. That is, the larger the pore size of the unfired compact, the wider was the pore size distribution and the higher was the pore growth rate during sintering. As the unfired microstructure depended on the powder preparation process, granule characteristics may be inferred to markedly influence the sintering process at low temperature.

Table 2
True porosity of the unfired and fired SD, DPGP, and G compacts pressed at different pressures to constant dry bulk density (2.00 g/cm^3).

	Unfired	1000 °C	1050 °C	1100 °C
SD (32.5 MPa)	0.250 ± 0.007	0.263 ± 0.006	0.252 ± 0.006	0.225 ± 0.007
DPGP (29.0 MPa)	0.248 ± 0.006	0.272 ± 0.007	0.251 ± 0.005	0.225 ± 0.007
G (15.5 MPa)	0.251 ± 0.005	0.273 ± 0.008	0.248 ± 0.006	0.224 ± 0.006

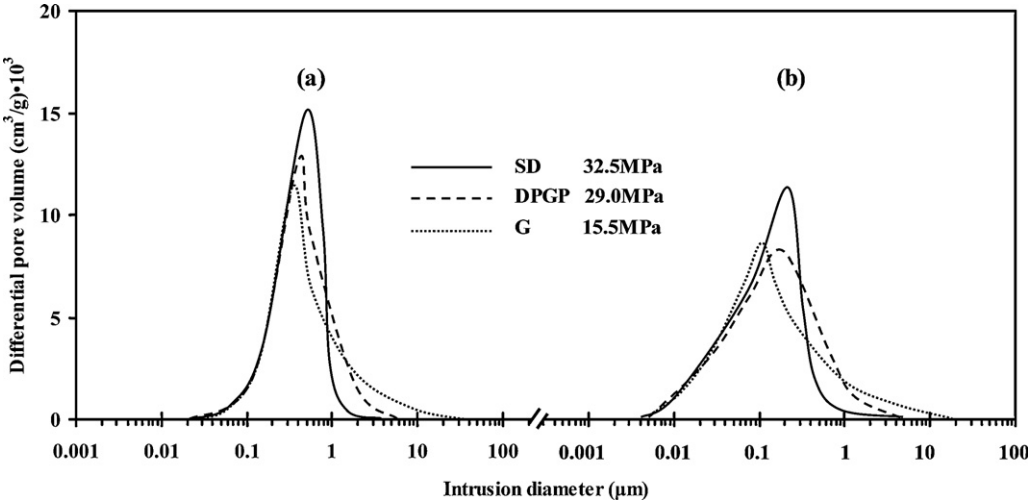

Fig. 2. Pore size distribution of (a) the SD, DPGP, and G compacts fired at 1100 °C and (b) their unfired compacts.

3.1.2. Properties of the fired compacts

Bulk density (BD) and apparent porosity, expressed as water absorption (WA), have been plotted versus firing temperature of the SD, DPGP, and G compacts fired at higher temperatures (1180–1240 °C) in Fig. 4. The figure shows that the three compacts reached the highest maximum bulk density at a similar temperature ($T_{max} \sim 1210$ °C). The SD compact achieved the highest maximum bulk density (2.37 g/cm^3) of the three compacts at T_{max}, cancelling out apparent porosity, whereas the G compact achieved the lowest maximum bulk density (2.31 g/cm^3) and had the highest apparent porosity (WA = 1.82%) at T_{max}. The DPGP compact displayed an intermediate behaviour (BD = 2.35 g/cm^3 and WA = 1.38%). The fact that certain compacts exhibited water absorption at T_{max} (DPGP and particularly G) indicates that the porous system was partially connected.

These differences were related to the large pores (d_{16}) in the unfired compacts. As observed above in Fig. 3, the pore size of the unfired compacts and large pore (d_{16}) growth rate increased in the order SD, DPGP, and G. Since larger pores are harder to eliminate by liquid-phase formation in firing, the densification and vitrification rates (slopes of the BD–T and WA–T curves in Fig. 4) and the final degree of densification and vitrification (values of BD and WA at T_{max} in Fig. 4) decreased in the order SD, DPGP, and G.

Fig. 5 shows the porous microstructure of the SD, DPGP, and G compacts fired at T_{max} and subsequently polished. The fired SD and DPGP compacts displayed a similar microstructure, mainly consisting of pores smaller than 20 μm in addition to a few large pores (about 100 μm). According to the literature [14], the presence of large pores in fired porcelain tiles prepared from spray-dried powder is related to the inner void in the spray-dried powder granules. These voids remain in the pressed green compacts owing to insufficient granule deformation and they grow during firing. A previous study [7] showed that the DPGP granules also had large inner voids (>20 μm), which originated during the rolling treatment of the DPGP granulation process, so that these inner voids might generate large pores in the DPGP compacts during firing.

The fired G compact exhibited a different microstructure, with many very large pores (about 200 μm) between the remaining granule boundaries. The low deformability of the G granules (absence of inner voids) led to numerous large intergranular pores in the pressed green compacts, as observed elsewhere [7]. These pores could not be eliminated during firing and gave rise to very large pores in the fired compacts.

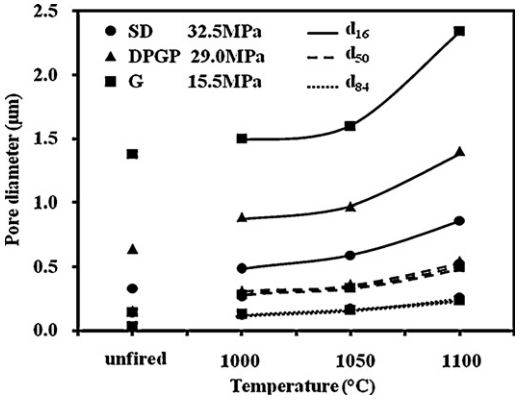

Fig. 3. Variation of statistical parameters d_{16}, d_{50}, and d_{84} with firing temperature.

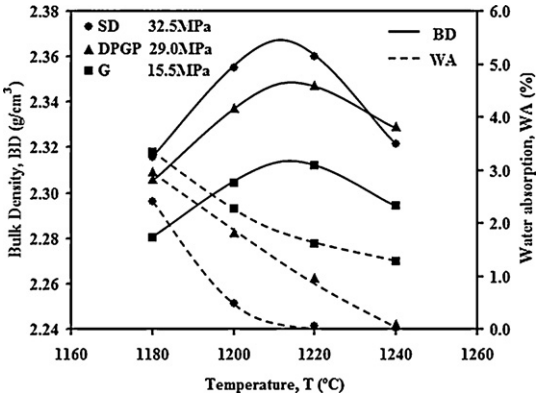

Fig. 4. Variation of bulk density and water absorption with firing temperature.

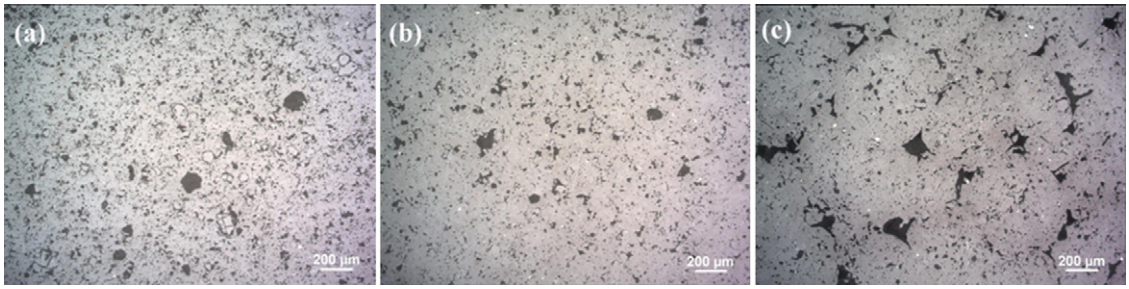

Fig. 5. Polished cross-sections (BF images) of the (a) SD, (b) DPGP, and (c) G compacts fired at T_{max}.

Initial and final dirt retention of the polished compacts fired at T_{max} are plotted in Fig. 6. The figure shows that dirt retention (initial and final) increased in the order SD, DPGP, and G owing to the increase in porosity (Fig. 4) and pore interconnectivity (evaluated as water absorption) of the fired compacts, in the same order.

These results indicate that, starting from the same unfired bulk density, the compacts fired at T_{max} exhibited increasing porosity, pore size, and pore connection in the order SD < DPGP < G. These differences were related to granule deformation at the pressing pressures used (32.5, 29.0, and 15.5 MPa, respectively, for the SD, DPGP, and G granules), granule deformation increasing in the opposite order. The largest pores in the unfired compacts thus adversely affected compact densification and vitrification during firing and impaired polished compact stain resistance. Granule deformation during pressing, therefore, needs to be enhanced in order to improve porcelain tile densification and vitrification.

3.2. Compacts pressed at the same pressing pressure (32.5 MPa)

3.2.1. Evolution of compact microstructure with firing temperature

The pore size distributions of the unfired and fired DPGP, G, and NG compacts, pressed at the same pressure (32.5 MPa), are shown in Fig. 7. Those of the SD compacts are depicted in Fig. 1. Table 3 details the true porosity of the compacts.

The same tendency as that observed in Fig. 1 and Table 2 is exhibited in Fig. 7 and Table 3: when temperature increased, porosity decreased and pore size distribution shifted progressively towards larger pore sizes in each type of compact, which agrees with the results of Section 3.1.1.

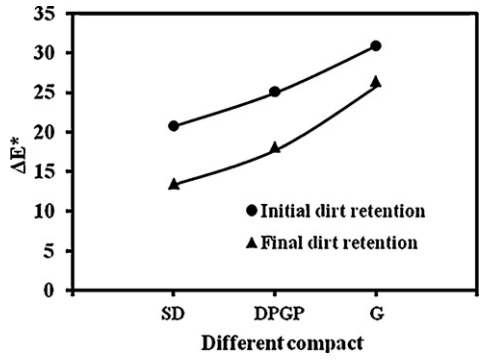

Fig. 6. Dirt retention of the polished compacts fired at T_{max}.

In order to analyse the influence of the powder preparation process, the pore size distributions of the SD, DPGP, G, and NG compacts fired at 1100 °C were plotted in Fig. 8a. The figure shows that there was a great difference between the pore size distribution of the non-granulated powder (NG) compact and the pore size distributions of the granulated powder (SD, DPGP, and G) compacts, the latter pore size distributions resembling each other more closely. The NG compact exhibited a narrower pore size distribution with fewer small pores (<1 μm) and more numerous large pores (>1 μm) than the SD, DPGP, and G compacts. In the three granulated powder compacts, the quantity and size of the large pores (1–10 μm) increased in the order SD, G, and DPGP.

These differences were also found in the porosity distributions of the unfired compacts (Fig. 8b) and the compacts fired at 1000 °C and 1050 °C (figures omitted). This indicates that the difference in pore size between the unfired compacts pressed from different types of powders persisted after sintering (at least up to 1100 °C), highlighting the importance of the powder preparation process in the pore size distribution of the fired compacts, which is consistent with the results of Section 3.1.1.

The significant difference in pore size distribution between that of the NG compacts and those of the SD, DPGP, and G compacts is deemed to stem from the absence of a granulation step in the NG powder preparation process. For the SD, DPGP, and G compacts, the raw material particles were first compacted to form granules during the granulation step according to different mechanisms [7]. The granules were then, in turn, compacted by pressing to obtain the green test pieces. In contrast, in the NG compacts, the raw material particles were compacted directly by pressing to form green compacts, without a pre-compacting (granulation) process.

The granules obtained by the three granulation processes displayed a pore size range between 0.01 and 1 μm [7], which was the same as most of the pore size ranges in the unfired test compacts (Fig. 8b). This indicates that the pressing stage at 32.5 MPa partially eliminated the intergranular pores and inner voids but scarcely eliminated the intragranular pores, highlighting the significant contribution of the granulation step to raw material particle compaction. In contrast, the unfired compacts pressed from the NG powder without a granulation step exhibited fewer small pores (<0.2 μm) and many more

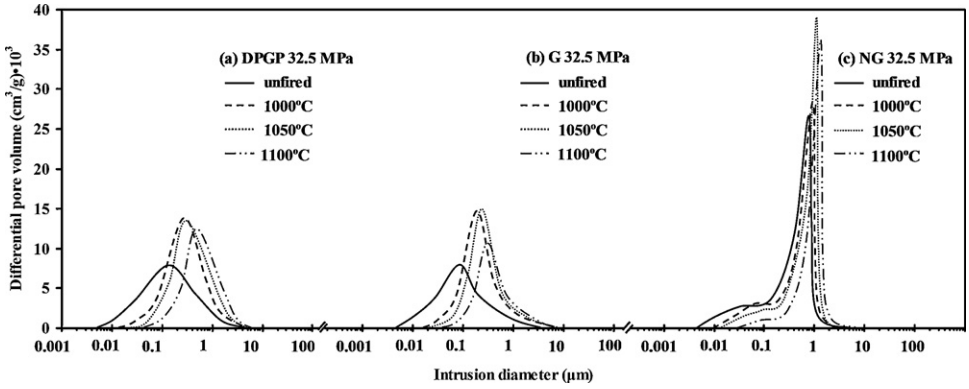

Fig. 7. Pore size distribution of the unfired and fired (a) DPGP, (b) G, and (c) NG compacts pressed at the same pressure 32.5 MPa.

Table 3
True porosity of the unfired and fired SD, DPGP, G, and NG compacts pressed at the same pressure 32.5 MPa.

	Unfired	1000 °C	1050 °C	1100 °C
SD (32.5 MPa)	0.261 ± 0.005	0.284 ± 0.007	0.258 ± 0.007	0.233 ± 0.006
DPGP (32.5 MPa)	0.243 ± 0.005	0.261 ± 0.006	0.258 ± 0.008	0.234 ± 0.006
G (32.5 MPa)	0.212 ± 0.007	0.243 ± 0.009	0.225 ± 0.007	0.185 ± 0.005
NG (32.5 MPa)	0.307 ± 0.008	0.315 ± 0.007	0.298 ± 0.006	0.274 ± 0.006

large pores (0.2–2 μm) (Fig. 8b). In addition, the unfired NG compacts displayed higher true porosity than the three granulated powders (Table 3). The differences in porosity between the unfired test pieces pressed from the non-granulated and from the granulated powders showed that the granulation step significantly contributed to reducing porosity and pore sizes in the unfired compacts.

In order to further analyse the evolution of porosity during sintering, the values of d_{16}, d_{50}, and d_{84} of the four different studied compacts were plotted versus firing temperature in Fig. 9. Pore size of the unfired compacts and the pore growth rate (curve slope) of the small (d_{84}) and medium (d_{50}) pores both increased in the same order G, SD, DPGP, and NG, again indicating that the larger pores grew faster. However, a disagreement was found in the case of the large pores (d_{16}): though the large-pore size of the unfired NG compact was much higher than that of the unfired SD, DPGP, and G compacts, the growth rate of the NG large pores was similar to that of the SD and G compacts.

In order to better understand this, the compact microstructures were examined by scanning electron microscopy (SEM). Fig. 10 shows the SEM microstructure of the four studied unfired compacts. The unfired NG compact displayed a uniform microstructure, whereas the unfired SD, DPGP, and G compacts exhibited many excessively large pores (much bigger than 10 μm). Those large pores had not been identified in the porosity distribution curves determined by mercury intrusion (Fig. 8b) as a result of the 'bottleneck' effect: that is, mercury filled the large pores through the smaller pores (bottlenecks) connecting the large pores to the outside, so that the intrusion

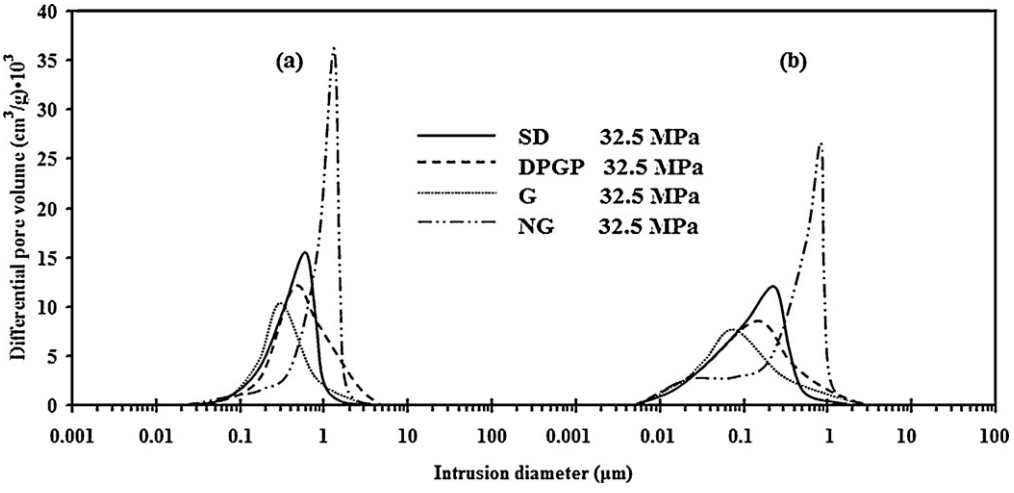

Fig. 8. Pore size distribution of (a) the SD, DPGP, G, and NG compacts fired at 1100 °C and (b) their unfired compacts.

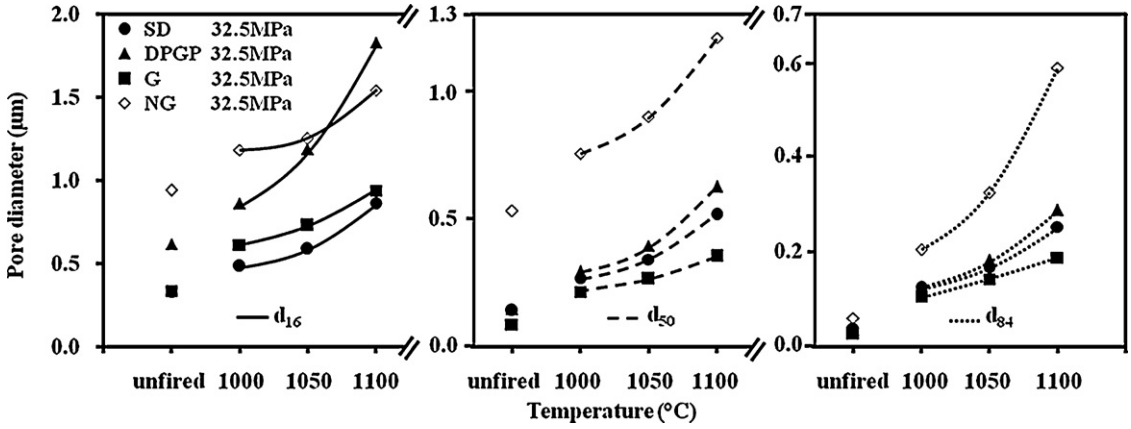

Fig. 9. Variation of statistical parameters d_{16}, d_{50}, and d_{84} with firing temperature.

volume of the large pores was based on the bottleneck diameter. Such large pores have seldom been reported in previous studies on porcelain tiles [2,3,14], though they significantly contribute to porcelain tile final porosity.

These pores are assumed to be the intergranular pores and the voids that remained inside the SD and DPGP granules, owing to insufficient granule deformation during pressing. The NG compacts were pressed from non-granulated powder and were, hence, free of large intergranular pores. In view of the excessively large pores, the real size of the large pores (d_{16}) of the SD, DPGP, and G compacts may be assumed to have been much higher than those shown in Fig. 9, leading to the higher large-pore growth rate observed.

3.2.2. Properties of the fired compacts

Bulk density and apparent porosity, expressed as water absorption, have been plotted versus firing temperature for the SD, DPGP, G, and NG compacts fired at higher temperatures (1180–1240 °C) in Fig. 11. The figure shows that the four

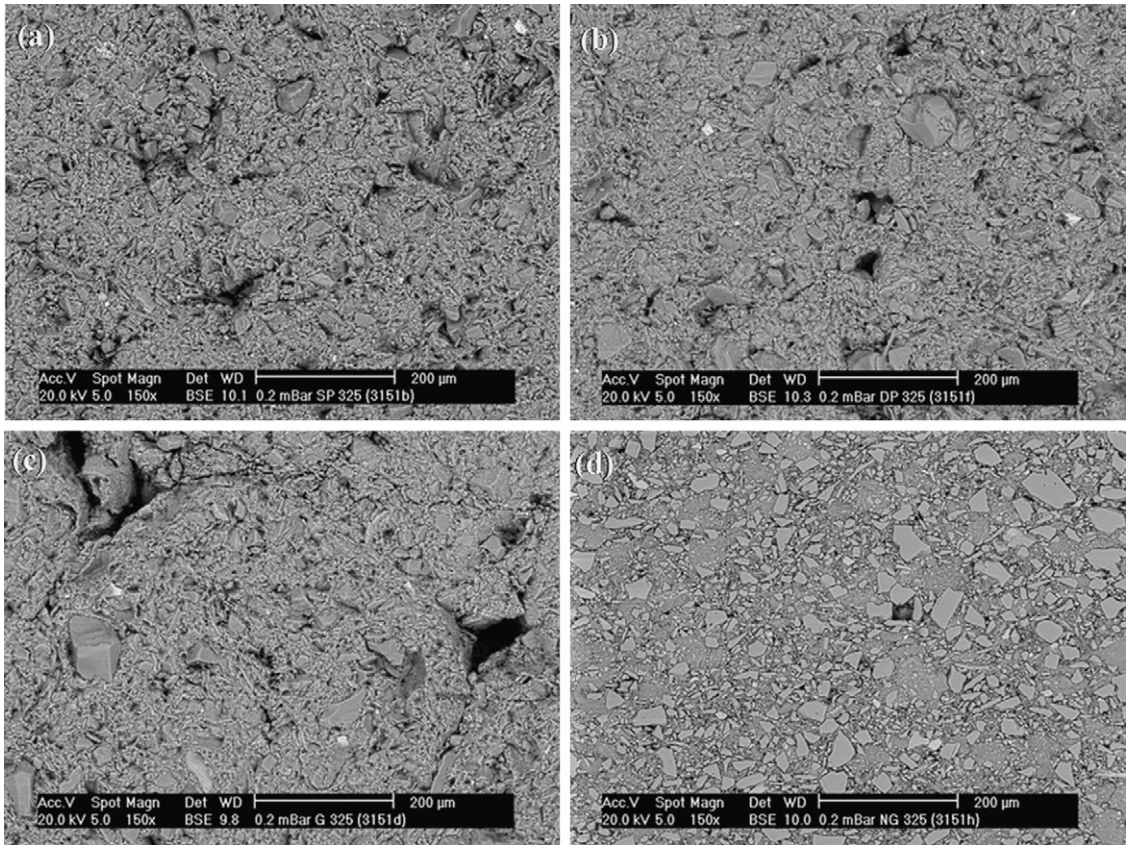

Fig. 10. Microstructure of the unfired (a) SD, (b) DPGP, (c) G, and (d) NG compacts.

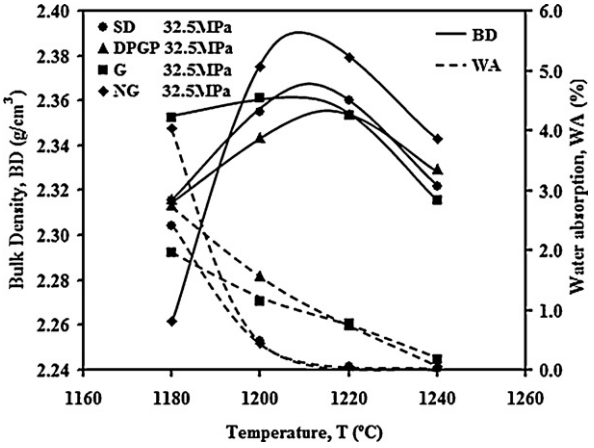

Fig. 11. Variation of bulk density and water absorption with firing temperature.

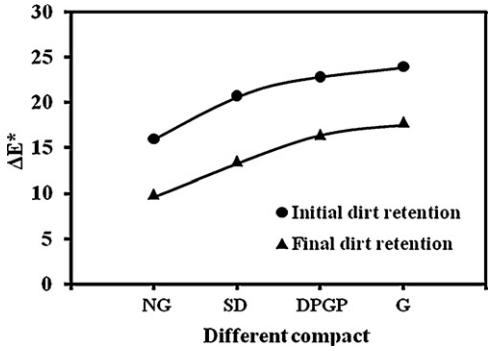

Fig. 13. Dirt retention of the polished compacts fired at T_{max}.

studied compacts needed a similar temperature (T_{max}, ~1210 °C) to reach the highest maximum bulk density.

In the compacts prepared from the granulated powders (SD, DPGP, and G), the SD compact achieved the highest maximum bulk density (2.37 g/cm^3) at T_{max}, the G compact attaining an intermediate maximum bulk density (2.36 g/cm^3), and the DPGP compact achieving the lowest maximum bulk density (2.35 g/cm^3). In view of the difference in total pore volume (Table 3) and pore size (Fig. 8b) of the unfired compacts, compact densification degree at T_{max} is assumed to depend more on pore size than on pore volume: the densification degree increased as pore size of the unfired compact decreased, in accordance with the results obtained in Section 3.1.2. Moreover, at T_{max}, the SD compact cancelled out apparent porosity, while the G and DPGP compacts retained an apparent porosity (WA = 0.96% and 1.10% respectively), again indicating that the larger unfired pores were harder to close and led to poorer vitrification.

It may be noted that, in comparison with the SD, DPGP, and G compacts, though the NG compact started from a much higher total pore volume (Table 3) and larger pore size according to Fig. 8b, it ultimately reached the highest maximum bulk density and cancelled out apparent porosity at T_{max}.

Fig. 12 shows the porous microstructure of the DPGP, G, and NG compacts fired at T_{max} and subsequently polished; that of the SD compact is shown in Fig. 5. It may be observed that the NG compact (Fig. 12a) had a uniform microstructure without large pores, while the SD, DPGP, and G compacts exhibited large pores, particularly the G compact (Fig. 12c) in which the remaining granule boundaries were evident. The same trend was also found in the microstructures of the unfired compacts (Fig. 10). These results indicate that the key pores in the unfired compacts adversely affecting the densification and vitrification process were not the large pores of about 0.2–2 μm shown in the porosity distribution curves determined by mercury intrusion (Fig. 8b), but the excessively large pores bigger than 10 μm only observed by SEM (Fig. 10).

It may, therefore, be noted once again that, in order to produce porcelain tile with excellent densification and vitrification from granulated powder, attention should particularly be paid to raising granule deformability and, thus, reducing the size of the intergranular pores remaining in the unfired compacts.

Initial and final dirt retention of the polished compacts fired at T_{max} are plotted in Fig. 13. The figure shows that dirt retention (initial and final) increased in the order NG, SD, DPGP, and G owing to the increase in the porosity (Fig. 11) and pore size (Fig. 12) of the fired compacts, in the same order.

It may be assumed, therefore, that the excessively large pores (bigger than 10 μm) in the unfired compacts, identified by optical observation but not by mercury intrusion porosimetry, constituted the residual porosity and impaired compact densification and vitrification during sintering,

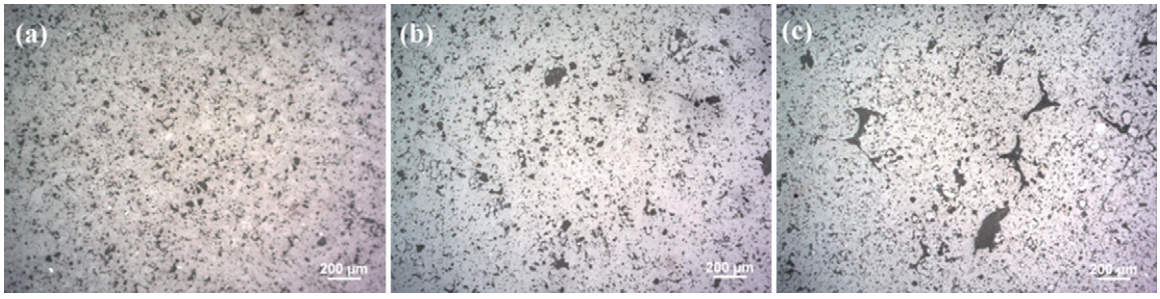

Fig. 12. Polished cross-sections (BF images) of the (a) NG, (b) DPGP, and (c) G compacts fired at T_{max}.

thus leading to poorer stain resistance of the polished compacts.

4. Conclusions

The firing behaviour and fired properties of compacts formed by pressing from four different types of powders were studied. Three granulated powders, respectively obtained by the novel droplet-powder granulation process (DPGP), the traditional spray-drying (SD) process, and the granulation (G) process, and a non-granulated powder (NG) obtained by dry milling were used.

The study shows that pressing powder characteristics, especially granule deformability and granule pore structure, defined the microstructure of the unfired compacts, which was in turn responsible for the sintering behaviour and properties of the fired compacts.

The study shows, furthermore, that the DPGP improved the sintering behaviour and final properties of the resulting porcelain tiles with respect to those obtained by the G process when operating at constant bulk density of the unfired compacts, constant unfired bulk density being the typical situation in industrial practice. However, the fired compacts prepared from the DPGP powder exhibited a higher porosity and pore size compared with those of the compacts obtained from the SD granules. This was due to the lower deformability of the DPGP granules compared with that of the SD granules.

These results confirm the complexity of porcelain tile manufacturing processes with a granulation step, given the difficulty of achieving the required tile water absorption ($<0.5\%$) before the tiles start bloating.

The new (DPGP) process opens up the possibility of manufacturing glazed porcelain tiles with a more eco-friendly process. However, the results also indicate that polished porcelain tile manufacture by the DPGP requires further research in order to improve granule characteristics. The findings indicate, in particular, that green granule deformability is the critical factor and that granule deformability needs to be enhanced to facilitate porcelain tile densification and vitrification during firing, in order to match the tile stain resistance achieved with the SD powder.

Acknowledgements

This study has been conducted in the frame of an International Cooperation between the China University of Geosciences (CUG, China) and the Instituto de Tecnología Cerámica (ITC) at Universitat Jaume I (UJI, Spain). The Chinese Scholarship Council is also gratefully thanked for its financial support (File No. 2009641029).

References

[1] E. Sanchez, J. García-Ten, V. Sanz, A. Moreno, Porcelain tile: almost 30 years of steady scientic-technological evolution, Ceram. Int. 36 (2010) 831–845.
[2] H.J. Alves, F.G. Melchiades, A.O. Boschi, Effect of spray-dried powder granulometry on the porous microstructure of polished porcelain tile, J. Eur. Ceram. Soc. 30 (2010) 1259–1265.
[3] J.L. Amoros, M.J. Orts, J. Garcia-Ten, A. Gozalbo, E. Sanchez, Effect of the green porous texture on porcelain tile properties, J. Eur. Ceram. Soc. 27 (2007) 2295–2301.
[4] K. Darcovich, F. Toll, P. Hontanx, V. Roux, K. Shinagawa, An experimental and numerical study of particle size distribution effects on the sintering of porous ceramics, Mater. Sci. Eng. 348 (2003) 76–83.
[5] P.M.T. Cavalcante, M. Dondi, G. Ercolani, G. Guarini, C. Melandri, M. Raimondo, R.E. Almendra, The inuence of microstructure on the performance of white porcelain stoneware, Ceram. Int. 30 (2004) 953–963.
[6] Z. Shu, J. Zhou, Y.X. Wang, A novel approach of preparing press-powders for cleaner production of ceramic tiles, J. Clean. Prod. 18 (2010) 1045–1051.
[7] Z. Shu, J. Garcia-Ten, E. Monfort, J.L. Amoros, J. Zhou, Y.X. Wang, Cleaner production of porcelain tile powders. Granule and green compact characterization, Ceram. Int. (2011), doi:10.1016/j.ceramint.2011.07.037.
[8] J. Brakel, S. Modry, M. Svata, Mercury porosimetry: state of the art, Powder Technol. 29 (1981) 1–12.
[9] M.J. Orts, A. Escardino, J.L. Amorós, F. Negre, Microstructural changes during the ring of stoneware oor tiles, Appl. Clay Sci. 8 (1993) 231–245.
[10] R.S. Hunter, R.W. Harold, The Measurement of Appearance, John Wiley & Sons, New York, 1987.
[11] R. Toledo, D.R. dos Santos, R.T. Faria Jr., J.G. Carrió, L.T. Auler, H. Vargas, Gas release during clay firing and evolution of ceramic properties, Appl. Clay Sci. 27 (2004) 151–157.
[12] M.D. Sacks, T.Y. Tseng, Preparation of SiO_2 glass from model powder compacts. Part 2. Sintering, J. Am. Ceram. Soc. 67 (1984) 532–537.
[13] M.D. Sacks, T.Y. Tseng, Preparation of SiO_2 glass from model powder compacts. Part 3. Enhanced densication by sol inltration, J. Am. Ceram. Soc. 71 (1988) 245–249.
[14] J. García-Ten, E. Sanchez, G. Mallol, J.C. Jarque, A. Arroyo, Influence of operating variables on spray-dried granule and resulting tile characteristics, Key Eng. Mater. 264–268 (2004) 1499–1502.